Communication

Application of Quenching and Partitioning Processing to Medium Mn Steel

EUN JUNG SEO, LAWRENCE CHO,
and BRUNO C. DE COOMAN

The present work analyzes the application of quenching and partitioning processing to medium Mn steel to obtain a new type of ultra-high-strength multiphase medium Mn steel. The selection of the quench temperature makes it possible to vary the ultimate tensile strength within a range of 500 MPa. The processing leads to low-carbon lath martensite matrix with a controlled volume fraction of retained austenite.

Increasing requirements related to passenger safety and weight reduction in the automotive industry have led to the development of a first generation of advanced high strength steels (AHSS) such as dual phase and transformation-induced plasticity (TRIP) steels. Second generation austenitic high-Mn twinning-induced plasticity (TWIP) steel with a Mn content in the range of 15 to 25 wt pct exhibits an excellent combination of tensile strength (~1 GPa) and ductility (~60 pct) due to a dynamic Hall–Petch effect resulting from the gradual increase of the density of mechanical twins during deformation.[1,2] The higher alloying costs and the lower productivity associated with high-Mn TWIP steel are currently the main drivers behind the development of the intermediate and medium Mn steel. Adequate combinations of mechanical properties have been reported for intercritically annealed intermediate and medium Mn steels. Their high work-hardening rate is achieved by the TRIP effect or a combination of two plasticity-enhancing mechanisms, the TWIP effect and the TRIP effect.[3–5] The Mn content in these materials is typically one third of the Mn content of the high-Mn TWIP steels, but despite their lower Mn content, these steels achieve excellent mechanical properties with a strength-ductility balance in the range of 35,000 to 45,000 MPa pct.

Quenching and partitioning (Q&P) processing was proposed by Speer *et al.*[6] as a new approach to produce steel microstructures consisting of a low-C martensitic matrix containing a considerable volume fraction of retained austenite. Earlier studies have shown that the Q&P processing of various AHSS enables the use of the TRIP effect to achieve a pronounced improvement of mechanical strength and ductility.[7–9]

The Q&P processing consists of three stages: an initial quenching stage, a partitioning stage, and a final quenching stage. The austenitized steel is initially quenched to a temperature, T_Q, in the $M_s - M_f$ temperature range, and partially transformed to primary martensite. It is then partition treated at the partitioning temperature, T_P. During the partitioning stage, C diffuses from the supersaturated primary martensite into the untransformed austenite. As a result, the M_s temperature of the C-enriched austenite is lowered. This leads to the stabilization of the untransformed austenite upon cooling to room temperature. If C does not partition enough to austenite, some of the austenite will transform to secondary martensite in the final quenching stage. The final microstructure consists of C-enriched austenite islands in a low-C lath martensite matrix. The martensite contributes a high strength level to the material and the C-enriched austenite enhances the elongation and the toughness. The compositions of Q&P steels are lean, consisting mostly of C, Mn, and Si. C and Mn are well known to enhance the austenite stability. Addition of Si allows C partitioning to austenite by suppressing the carbide precipitation during the partitioning stage.[10] In the present work, the application of the Q&P processing concept was analyzed for medium Mn steel for the first time.

The chemical composition of the medium Mn steel was Fe-0.21C-4.0Mn-1.6Si-1.0Cr (in wt pct). The M_s temperature of the steel was 546 K (273 °C). The synergetic effect of the Si and Cr additions in increasing the retained austenite volume fraction during Q&P processing was reported previously.[8,11] The microstructure of the industrially cold-rolled sheet steel prior to Q&P processing was a complex microstructure containing deformed pearlite and martensite.

Q&P processing was carried out in a Bähr 805 pushrod dilatometer either in vacuum or in a He atmosphere. The specimens with dimensions of $10 \times 5 \times 1.2$ mm^3 were heated at a heating rate of +10 °C/s to 1123 K (850 °C), fully austenitized for 240 seconds at 1123 K (850 °C) and initially quenched to a T_Q temperature in the range of 423 K to 543 K (150 °C to 270 °C) with 293 K (20 °C) increments. Subsequently, the specimens were reheated to the partitioning temperature (T_P) using a heating rate of +20 °C/s, held at the T_P temperature for 300 seconds, and finally quenched to room temperature. The initial and final quenching was done using He gas to obtain a cooling rate of −50 °C/s.

The volume fraction of retained austenite was measured by a METIS magnetic saturation device. The C content of retained austenite was measured by means of XRD measurements, using a Bruker D8 Advance X-ray diffractometer equipped with a Cu tube. The austenite lattice parameter was determined by the Nelson–Riley method.[12]

EUN JUNG SEO and LAWRENCE CHO, Graduate Students, and BRUNO C. DE COOMAN, Professor and Director, are with the Materials Design Laboratory, Graduate Institute of Ferrous Technology, Pohang University of Science and Technology, Pohang 790-784, South Korea. Contact e-mail: decooman@postech.ac.kr

The microstructure of the Q&P-processed medium Mn steel was observed by means of scanning electron microscopy and electron backscattering diffraction (EBSD) conducted in a FEI Quanta 3D FEG. All the specimens used for the microstructural analysis and the XRD measurements were prepared by electro-chemical polishing in a solution of 5 pct $HClO_4$ + 95 pct CH_3COOH in order to minimize possible errors originating from the mechanically induced transformation of retained austenite during sample preparation. Cross-sectional transmission electron microscopy (TEM) specimens were also prepared by the Focused Ion Beam technique in a FEI Quanta 3D FEG. The cross-sectional TEM specimens were analyzed in a JEOL JEM-2100F FE-TEM operating at 200 keV.

ASTM E8 standard sub-size tensile specimens with a gage length of 25 mm were prepared as follows. Using a box furnace, the specimens were fully austenitized at 1123 K (850 °C) for 240 seconds and initially quenched in an oil bath ($T_Q < 240$ °C) or in a salt bath ($T_Q > 240$ °C), prior to reheating to 723 K (450 °C) in a salt bath for the partitioning stage. The specimens were then water quenched to room temperature. The mechanical properties of the specimens were measured with a Zwick/Roell universal tensile testing machine.

Each specimen was cut into 5-mm segments at 10-mm intervals from the fracture to measure the volume fraction of deformation-transformed austenite after the

tensile test. The retained austenite fraction of these specimens was measured by magnetic saturation.

The applicability of the Q&P concept to medium Mn steel was investigated by dilatometry. Figure 1 shows the dilatometry traces for the Q&P-processed medium Mn steel. For the specimens quenched to T_Q in the range of 423 K to 483 K (150 °C to 210 °C), there was no volume expansion during the final quenching, i.e., no secondary martensite was formed. This implies that the C enrichment of austenite at the end of the partitioning stage was large enough to suppress its transformation to martensite in the final quenching stage. On the other hand, for the specimens quenched to a T_Q temperature in the range of 503 K to 543 K (230 °C to 270 °C), a volume expansion due to the transformation of austenite into α' martensite was clearly observed during the final quenching stage. The fact that the volume expansion during the final quenching increased with increasing T_Q temperature, implies that the stability of the austenite prior to the final quenching decreased with increasing T_Q.

Figure 2a shows the volume fraction of retained austenite, V_γ, as a function of T_Q. As T_Q increased, V_γ initially increased up to 0.33. For T_Q temperatures above 483 K (210 °C), V_γ gradually decreased. The T_Q temperature at which the maximum austenite fraction was obtained, $T_{Q,max}$, was 483 K (210 °C). It is clearly shown in Figure 1 that the decrease of V_γ at higher $T_{Q,max}$ results from the formation of secondary martensite. The stability of the austenite was lower when the steel was quenched to a higher T_Q because of an insufficient C enrichment. This is due to the fact that V_γ increased with increasing T_Q. The amount of C partitioned per unit volume of austenite is lower for larger values of V_γ. The result is a less stable retained austenite.

In order to investigate the stability of the retained austenite, the retained austenite C content, C_γ, was measured. Figure 2(b) shows the T_Q dependence of C_γ. C_γ was determined by means of the room temperature measurement of the lattice parameter of the retained austenite, a_γ, and the following relationship[13,14] between the lattice parameter and the composition:

$$a_\gamma(nm) = 0.3556 + 4.53 \times 10^{-3}C + 9.5 \times 10^{-5}Mn$$
$$- 2.0 \times 10^{-5}Ni + 6.0 \times 10^{-5}Cr$$
$$+ 5.6 \times 10^{-4}Al + 3.1 \times 10^{-4}Mo + 1.8 \times 10^{-4}V$$

[1]

C_γ was in the range of 0.63 to 1.17 wt pct, which clearly shows that the C in the martensite partitioned into austenite during the Q&P processing. As T_Q increased, C_γ decreased and this resulted in lower austenite stability. The composition dependence of the M_s temperature is given by the following empirical relationship[15,16]:

$$M_s = 539 - 423\ C - 30.4\ Mn - 12.1\ Cr - 17.7\ Ni$$
$$- 7.50\ Mo + 10.0\ Co - 7.50\ Si$$

[2]

Here, the concentration of each alloy addition is in wt pct. Using Eq. [2], it can be shown that for the
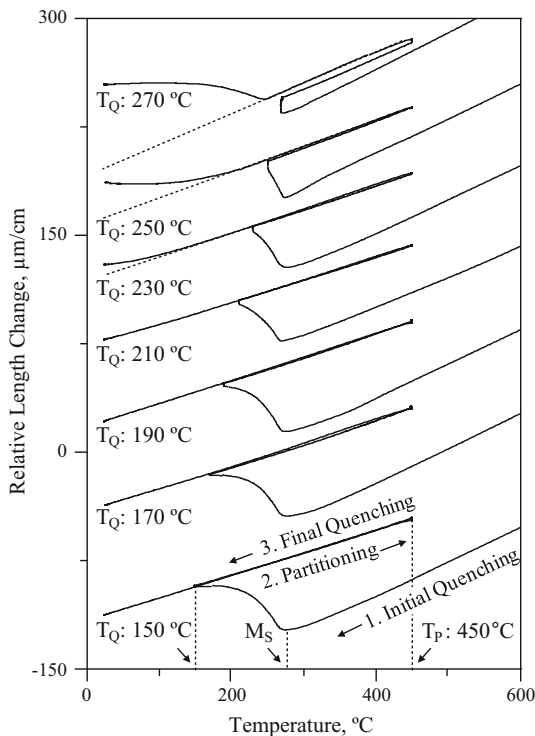

Fig. 1—Relative length change of dilatometry specimens of 4 wt pct medium Mn steel quenched (1. initial quenching) from 1123 K (850 °C) to different T_Q in the range from 423 K to 543 K (150 °C to 270 °C), and partition treated at a T_P of 723 K (450 °C) for 300 s (2. Partitioning). The volume expansion resulting from the formation of secondary martensite during the final quenching stage (3. final quenching) is indicated by the departure from the dotted line.

medium Mn steel used in the present study, the M_s temperature was below room temperature when C_γ exceeded 0.87 wt pct, indicating that austenite can be stabilized at room temperature. Figure 3(c) shows that the M_s temperature is below room temperature when $T_Q < 210$ °C. This clearly indicates that the formation of secondary martensite can be suppressed when a sufficiently high C_γ is obtained by Q&P processing with a T_Q temperature lower than 483 K (210 °C).
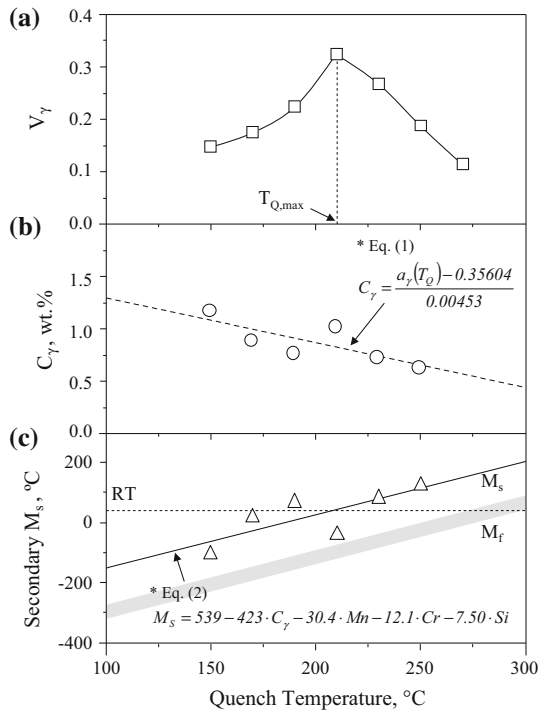

Fig. 2—(a) T_Q dependence of the volume fraction of retained austenite, V_γ, measured by the magnetic saturation method. (b) T_Q dependence of the retained austenite C content, C_γ, based on the XRD austenite lattice parameter measurements. The dashed line is based on the Eq. [1]. (c) T_Q dependence of the secondary M_s temperature of the C-enriched retained austenite. The solid line is based on Eq. [2].

Figure 3 shows the microstructure of the Q&P-processed medium Mn steel quenched to 483 K (210 °C) and partitioning treated at 723 K (450 °C) for 300 seconds. The microstructure of the Q&P-processed medium Mn steel consisted of a lath martensite matrix with retained austenite islands. The EBSD results in Figure 3(a) show that the austenite was present both as film-type and as blocky-type austenite. Figures 3(b) and 3(c) shows TEM micrographs of the Q&P-processed medium Mn steel. FCC and BCC diffraction patterns were obtained from retained austenite and martensite, respectively. The retained austenite could be clearly identified by means of dark-field imaging, as shown in Figure 3(c). The grain size of the retained austenite varied from 50 nm to 1 μm.

Figure 4 shows the mechanical properties of the Q&P-processed medium Mn steel quenched to a T_Q temperature in the range of 423 K to 543 K (150 °C to 270 °C) and partition treated for 300 seconds at 723 K (450 °C). The engineering stress–strain curves were continuous and no strain localization was observed. The mechanical properties of the Q&P-processed medium Mn steel could be divided into three types of behaviors depending on T_Q. Type-1 behavior was observed for specimens quenched to a low T_Q temperature (<210 °C). In this group, the specimens exhibited a high yield strength (YS) and total elongation (TE). The YS ranged from 1050 to 1160 MPa and the TE ranged from 15 to 18 pct. With increasing T_Q, the YS decreased slightly and the TE increased. This is due to the fact that V_γ increased for the Q&P-processed steel quenched at a higher T_Q temperature. These specimens exhibited a low work hardening, related to the stability of the retained austenite. When T_Q was equal to 423 K (150 °C), V_γ was 0.07 after the tensile test. This indicates that the stability of the retained austenite was high enough to suppress the strain-induced martensitic transformation. Type-2 behavior was observed for specimens quenched to the $T_{Q,max}$ (210 °C) temperature. This specimen had a relatively low YS and a high ultimate tensile strength (UTS) as compared to type-1 specimens. The low YS as compared to type-1 specimens is clearly due to a higher volume fraction of retained austenite, which is a much
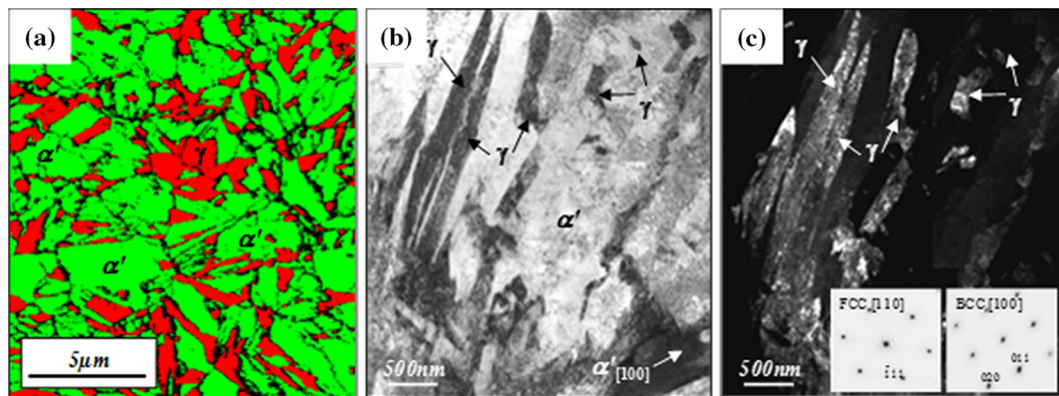

Fig. 3—Microstructure of Q&P-processed medium Mn steel obtained by austenitizing, quenching to 483 K (210 °C), and partitioning at 723 K (450 °C) for 300 s. (a) EBSD phase map for BCC (green) and FCC (red) phases. (b) Bright-field TEM micrograph. (c) Corresponding dark-field TEM micrograph of the retained austenite in (b) using the $(002)_\gamma$ reflection. γ and α represent retained austenite and martensite, respectively.
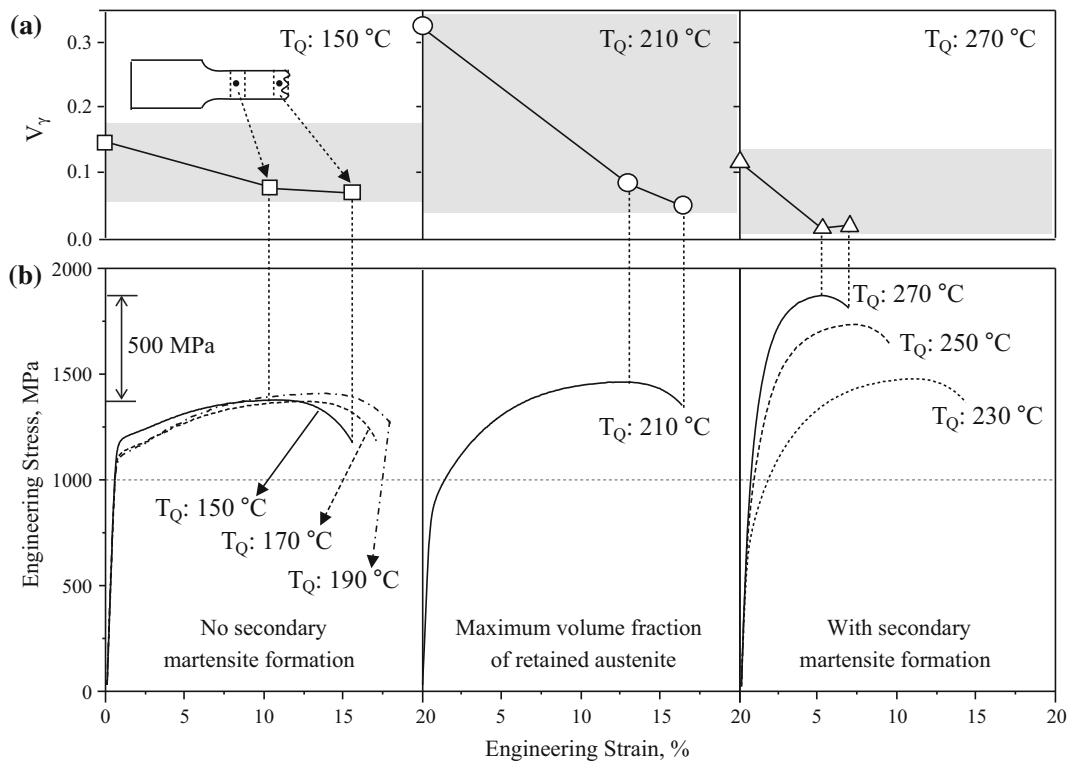
Fig. 4—(a) Volume fraction of retained austenite measured at 0 pct strain, at the onset of necking and at fracture. (b) Room temperature stress–strain curves for Q&P-processed medium Mn steel partition treated at 723 K (450 °C) for 300 s.

softer phase than martensite. The specimen exhibited a higher work-hardening rate resulting from the TRIP effect. Figure 4b clearly shows that a large amount of austenite transformed to martensite during tensile testing. Type-3 behavior was observed for specimens quenched to a high T_Q temperature (>210 °C). Secondary martensite formed during the processing of the specimens belonging to this group. These specimens exhibited an ultra-high UTS, but a low TE compared to specimens of the other two groups. The reason for this is clearly shown in Figure 4(a). In these specimen, most of the retained austenite transformed to martensite in the initial stage of the straining, resulting in high initial work-hardening rate. Another reason for the low TE of these specimens is the presence of the secondary martensite. As this is a high C brittle martensite, its presence resulted in a limited elongation. The mechanical properties of the secondary martensite formed during the final quenching are different from those of the primary martensite formed during initial quenching. The primary martensite contains a very low C content due to the C partitioning into the austenite, while secondary martensite is a highly C-enriched and extremely hard phase.

In conclusion, Q&P processing can successfully be applied to medium Mn steel to obtain ductile ultra-high-strength microstructures. Q&P processing of medium Mn steel resulted in a large volume fraction of C-enriched retained austenite, and a value of 0.33 was achieved. The microstructure of Q&P-processed medium Mn steel consisted of a low-C martensite matrix with C-enriched retained austenite islands. This microstructure had mechanical properties with an excellent strength-ductility balance of approximately 25,400 MPa pct. In addition, the selection of the quench temperature made it possible to vary the UTS over approximately 500 MPa in a controlled manner.

REFERENCES

1. B.C. De Cooman, O. Kwon, and K. Chin: *Mater. Sci. Technol.*, 2012, vol. 28, pp. 513–27.
2. C. Scott, S. Allain, M. Faral, and N. Guelton: *Revue de Métallurgie*, 2006, vol. 103, pp. 293–302.
3. S. Lee, S.-J. Lee, and B.C. De Cooman: *Acta Mater.*, 2011, vol. 59, pp. 7546–53.
4. H. Aydin, E. Essadiqi, I.-H. Jung, and S. Yue: *Mater. Sci. Eng., A*, 2013, vol. 564, pp. 501–08.
5. S. Lee and B.C. De Cooman: *Metall. Mater. Trans. A*, 2014, vol. 45A, pp. 709–16.
6. J.G. Speer, A.M. Streicher, D.K. Matlock, F. Rizzo, and G. Krauss: *Austenite Formation and Decomposition*, Warrendale, ISS/ TMS, 2003, pp. 505–22.
7. E. Paravicini Bagliani, M.J. Santofimia, L. Zhao, J. Sietsma, and E. Anelli: *Mater. Sci. Eng., A*, 2013, vol. 559, pp. 486–95.
8. H. Jirková, L. Kučerová, V. Průcha, and B. Mašek: *Proc. 21st Int. Conf. Metall. Mater. 2012*, TANGER Ltd., Brno Czech Republic, EU, 2012, pp. 532–38.
9. E. De Moor, J.G. Speer, D.K. Matlock, J.-H. Kwak, and S.-B. Lee: *ISIJ Int.*, 2011, vol. 51, pp. 137–44.
10. G. Miyamoto, J.C. Oh, K. Hono, T. Furuhara, and T. Maki: *Acta Mater.*, 2007, vol. 55, pp. 5027–38.

11. E.J. Seo, L. Cho, and B.C. De Cooman: *Metall. Mater. Trans. A*, 2014, vol. 45A, pp. 4022–37.
12. B.D. Cullity and S.R. Stock: *Elements of X-ray Diffraction*, Pearson, New Jersey, 2001, pp. 365–69.
13. D. Dyson and B. Holmes: *J. Iron Steel Inst.*, 1970, vol. 208, pp. 469–74.
14. N.H. van Dijk, A.M. Butt, L. Zhao, J. Sietsma, S.E. Offerman, J.P. Wright, and S. van der Zwaag: *Acta Mater.*, 2005, vol. 53, pp. 5439–47.
15. C. Kung and J. Rayment: *Metall. Mater. Trans. A*, 1982, vol. 13A, pp. 328–31.
16. K. Andrews: *J. Iron Steel Inst.*, 1965, vol. 203, pp. 721–27.